

刚性不对称三氮唑衍生物的 Cd(II)配合物的制备、 晶体结构及其荧光性质

徐周庆¹ 王晓宁¹ 李慧军^{*1} 贾磊^{*1} 赵惠子¹ 李守杰¹ 马录芳^{*2} 张培玲³

(¹ 河南理工大学物理化学学院, 焦作 454000)

(² 洛阳师范学院, 洛阳 471022)

(³ 河南理工大学电气学院, 焦作 454000)

摘要: 用水热法合成了基于刚性不对称三氮唑衍生物配体 H₂ptp (H₂ptp=4-(5-(1H-pyrazol-4-yl)-4H-1,2,4-triazol-3-yl)pyridine)的 2 个 Cd(II)配合物 $[\text{Cd}_2(\text{Hptp})_2(\text{OAc})_2] \cdot 7\text{H}_2\text{O}$ (**1**)和 $[\text{Cd}(\text{Hptp})\text{Cl}(\text{H}_2\text{O})] \cdot \text{H}_2\text{O}$ (**2**), 并通过元素分析、差热分析、粉末 X 射线衍射和单晶 X 射线衍射进行表征。配合物 **1** 具有一个梯状的一维结构, 在 $\pi \cdots \pi$ 堆积作用下这些一维梯链形成了超分子二维平面。在氢键的连接作用下, 客体水分子形成了独特的以双五元水簇为结构单元的水链, 这些水链填充在相邻的二维平面之间并通过氢键把二维平面连接成了三维超分子网络。配合物 **2** 具有一个新型的二维双层结构, 分子间氢键把这些二维平面连成了三维结构。另外, 测试了 2 个配合物的荧光性质。

关键词: 金属-有机框架; 荧光; 三氮唑衍生物

中图分类号: O614.24²

文献标识码: A

文章编号: 1001-4861(2016)07-1223-08

DOI: 10.11862/CJIC.2016.150

Syntheses, Crystal Structures and Luminescent Properties of Two Cd(II) Complexes Based on 4-(5-(1H-Pyrazol-4-yl)-4H-1,2,4-triazol-3-yl)pyridine

XU Zhou-Qing¹ WANG Xiao-Ning¹ LI Hui-Jun^{*1} JIA Lei^{*1}

ZHAO Hui-Zi¹ LI Shou-Jie¹ MA Lu-Fang^{*2} ZHANG Pei-Ling³

(¹Department of Physics and Chemistry, Henan Polytechnic University, Jiaozuo, Henan 454000, China)

(²College of Chemistry and Chemical Engineering, Luoyang Normal University, Luoyang, Henan 471022, China)

(³School of Electrical Engineering and Automation, Henan Polytechnic University, Jiaozuo, Henan 454000, China)

Abstract: Two new Cd(II) coordination polymers, namely $[\text{Cd}_2(\text{Hptp})_2(\text{OAc})_2] \cdot 7\text{H}_2\text{O}$ (**1**) and $[\text{Cd}(\text{Hptp})\text{Cl}(\text{H}_2\text{O})] \cdot \text{H}_2\text{O}$ (**2**), have been obtained through hydrothermal reaction of a new asymmetric rigid triazole derivatives H₂ptp (H₂ptp=4-(5-(1H-pyrazol-4-yl)-4H-1, 2,4-triazol-3-yl)pyridine) and cadmium salts. Complex **1** shows one dimensional (1D) ladder chain. Adjacent chains are further extended to a two dimensional (2D) supramolecular layer via $\pi \cdots \pi$ stacking interactions. Water chains comprised of double pentanuclear water cluster formed by hydrogen bonds were presented between the two layers. Complex **2** exhibits a unique 2D double layered motif which is further expanded to a 3D supramolecular structure through hydrogen bonding. Furthermore, the photoluminescence properties of these two complexes have been investigated in the solid state. CCDC: 1429655, **1**; 1415769, **2**.

Keywords: metal-organic frameworks; photoluminescence; triazole derivative

收稿日期: 2015-12-14。收修改稿日期: 2016-05-03。

国家自然科学基金(No.21404033, 21401046)、河南省科技攻关项目(No.152102210314)、河南省高等学校重点科研项目(No.16A150010)和河南理工大学博士基金(No.72103/001/103)资助。

*通信联系人。E-mail: lihuijunxy@hpu.edu.cn, mazhuxp@126.com, jlxj@hpu.edu.cn

0 Introduction

In recent decades, the rational design and construction of novel metal-organic frameworks (MOFs) has achieved chemist's great attentions not only for their intriguing variety of architectures and topologies, but also for stems from their potential applications in gas storage, luminescence, magnetism, and catalysis^[1-3]. Though numerous MOFs have been achieved, it still remains a long-term challenge to rationally and predictably prepare desired crystals^[4-5]. Generally, the resulting framework is mainly influenced by several factors, including the structural characteristics of ligands, the coordinated modes of centre metal ions, the solvent system, the counter-anions, and so on^[6-10]. In particular, the organic linkers plays crucial role in the construction of the targeted MOFs, because the ligand could adopt different conformations in the crystallization and further leads to structural isomerism. On this point, the suitable ligands selection is considerable significant to regulate and control the topology of coordination frameworks^[11-12].

As is well known, the triazole ring possessing aromaticity and variable coordination modes can afford multiple coordinating sites for linking closely situated metal ions to form complex with novel structure^[13-14]. In this context, a new type of triazole derivatives with the 3- and 5- sites substituted by two different azaheterocycles may be a good candidate because the multiple N atoms in this kind of ligands are more in favor of construction of MOFs with interesting structure and attractive properties. Taking these into account, 2-(3-(1*H*-pyrazol-4-yl)-1*H*-1,2,4-triazol-5-yl)pyridine (H_2ptp), an anisomeric triazole derivative, which contains one potential bidentate chelating site and three monodentate ones, was used as ligand to construct MOFs. Consequently, two novel Cd(II) coordination polymers, $\{[Cd_2(Hptp)_2(OAc)_2] \cdot 7H_2O\}_n$ (**1**) and $\{[Cd(Hptp)Cl(H_2O)] \cdot H_2O\}_n$ (**2**) had been obtained. These compounds are characterized by elemental analysis, IR spectra, and X-ray crystallography. In addition, their photoluminescent properties have also been investigated.

1 Experimental

1.1 Materials and measurements

All chemicals were commercially purchased and used without further purification. Elemental analyses for carbon, hydrogen and nitrogen were performed on a Thermo Science Flash 2000 element analyzer. FT-IR spectra were obtained in KBr disks on a Perkin Elmer Spectrum One FTIR spectrophotometer in 4 000~450 cm^{-1} spectral range. Solid-state (diffuse reflectance) electronic spectra were measured as polycrystalline samples on a Perkin Elmer Lambda2S spectrophotometer, within the range 400~1 100 nm. The powder X-ray diffraction (PXRD) analyses were performed with a Bruker AXS D8 Discover instrument (Cu $K\alpha$ radiation, $\lambda=0.154\ 184\ nm$) over the 2θ range of $5^\circ\sim 50^\circ$ at room temperature. Thermogravimetric analyses (TGA) were performed using a TG-DTA 2010S MAC apparatus between 30 and 500 $^\circ C$ in N_2 atmosphere with heating rate of $10\ ^\circ C \cdot min^{-1}$. The photoluminescent properties were measured on an F-4500 FL Spectrophotometer.

1.2 Preparations of the complexes 1 and 2

$\{[Cd_2(Hptp)_2(OAc)_2] \cdot 7H_2O\}_n$ (**1**). A mixture of H_2ptp (0.05 mmol, 10.60 mg), $Cd(OAc)_2 \cdot 2H_2O$ (0.10 mmol, 26.65 mg), absolute ethanol (5 mL) and H_2O (5 mL) was placed in a Teflon-lined stainless steel vessel (25 mL), heated to 120 $^\circ C$ for 3 days, and then cooled to room temperature at a rate of $5\ ^\circ C \cdot h^{-1}$. Yellow block crystals of **1** were obtained and picked out, washed with distilled water and dried in air. Yield: 16.5 mg, 56% (based on Cd). Elemental analysis Calcd. for $C_{24}H_{34}Cd_2N_{12}O_{11}$ (%): C 32.55, H 3.18, N 18.98; Found (%): C 32.15, H 3.08, N 18.87. IR (KBr, cm^{-1}): 3 244, 1 610, 1 550, 1 435, 1 355, 958, 754.

$\{[Cd(Hptp)Cl(H_2O)] \cdot H_2O\}_n$ (**2**). Complex **2** was synthesized in the similar way as that described for **1**, except that $Cd(OAc)_2 \cdot 2H_2O$ was replaced by $CdCl_2 \cdot 2H_2O$ (0.1 mmol, 20.13 mg). Colourless block crystals of **2** were obtained and picked out, washed with distilled water and dried in air. Yield: 15.3 mg, 63% (based on H_2ptp). Elemental analysis Calcd. for $C_{10}H_{11}CdClN_6O_2$ (%): C 30.39, H 2.80, N 21.27; Found(%): C

30.21, H 2.68, N 21.18. IR (KBr, cm^{-1}): 3 184, 1 629, 1 463, 1 435, 1 384, 947, 873.

1.3 X-ray crystallography

X-ray Single-crystal diffraction analyses of **1** and **2** were carried out on a Bruker SMART APEX II CCD diffractometer equipped with a graphite monochromated Mo $K\alpha$ radiation ($\lambda=0.071\ 073\ \text{nm}$) by using φ - ω scan technique at room temperature. The structures were solved via direct methods and successive Fourier difference synthesis and refined by the full-matrix least-squares method on F^2 with anisotropic thermal parameters for all non-H atoms (SHELXL-97)^[15-16]. The

empirical absorption corrections were applied by the SADABS program^[17]. The H-atoms of carbon were assigned with common isotropic displacement factors and included in the final refinement by the use of geometrical restraints. H-atoms of water molecules were first located by the Fourier maps and then refined by the riding mode. The crystallographic data for complexes **1** and **2** are listed in Table 1. Moreover, the selected bond lengths and bond angles are listed in Table 2 and Table 3.

CCDC: 1429655, **1**; 1415769, **2**.

Table 1 Crystal data and structure refinement details for complexes **1**~**2**

Complex	1	2
Formula	$\text{C}_{24}\text{H}_{34}\text{Cd}_2\text{N}_{12}\text{O}_{11}$	$\text{C}_{10}\text{H}_6\text{CdClN}_6\text{O}_2$
Formula weight	891.43	390.06
Crystal system	Triclinic	Monoclinic
Space group	$P\bar{1}$	$C2/c$
a / nm	0.902 8(3)	1.519 4(11)
b / nm	0.972 5(4)	1.528 6(11)
c / nm	1.063 4(4)	1.367 2(10)
$\alpha / (^\circ)$	84.027(5)	90
$\beta / (^\circ)$	72.615(6)	120.155(10)
$\gamma / (^\circ)$	88.451(6)	90
V / nm^3	0.886 1(6)	2.745 67(346)
Z	1	8
$D_c / (\text{g}\cdot\text{cm}^{-3})$	1.670	1.841
μ / mm^{-1}	1.270	1.794
Reflections collected, Unique (R_{int})	4 533, 3 088 (0.020 1)	7 131, 2 417 (0.029 7)
Data, restraints, parameters	3 088, 3, 221	2 417, 0, 181
Goodness-of-fit (GOF) on F^2	1.076	1.097
$R_1 [I > 2\sigma(I)]$	0.032 0	0.030 2
$wR_2 [I > 2\sigma(I)]$	0.076 9	0.080 8
R_1 (all data)	0.038 9	0.038 3
wR_2 (all data)	0.081 4	0.085 9

Table 2 Selected bonds (nm) and angles ($^\circ$) for **1**

Cd(1)-N(2)	0.227 2(2)	Cd(1)-N(3) ⁱ	0.228 4(2)	Cd(1)-O(2)	0.237 8(2)
Cd(1)-N(6) ⁱⁱ	0.231 7(2)	Cd(1)-N(1)	0.241 4(3)	Cd(1)-O(1)	0.242 65(18)
N(2)-Cd(1)-N(3) ⁱ	104.05(8)	N(2)-Cd(1)-N(6) ⁱⁱ	120.86(7)	N(3) ⁱ -Cd(1)-N(6) ⁱⁱ	89.88(8)
N(2)-Cd(1)-O(2)	135.30(7)	N(3) ⁱ -Cd(1)-O(2)	100.46(7)	N(6) ⁱⁱ -Cd(1)-O(2)	95.74(7)
N(2)-Cd(1)-N(1)	71.94(8)	N(3) ⁱ -Cd(1)-N(1)	175.55(7)	N(6) ⁱⁱ -Cd(1)-N(1)	90.64(8)
O(2)-Cd(1)-N(1)	83.88(7)	N(2)-Cd(1)-O(1)	88.27(7)	N(3) ⁱ -Cd(1)-O(1)	91.49(7)
N(6) ⁱⁱ -Cd(1)-O(1)	149.50(7)	O(2)-Cd(1)-O(1)	54.09(7)	N(1)-Cd(1)-O(1)	90.30(7)

Symmetry transformations used to generate equivalent atoms: ⁱ $x, 1+y, z$; ⁱⁱ $x, -1+y, z$

Table 3 Selected bonds (nm) and angles ($^{\circ}$) for **2**

Cd(1)-N(2)	0.226 9(3)	Cd(1)-Cl(1)	0.251 51(16)	Cd(1)-N(6) ⁱ	0.228 6(3)
Cd(1)-Cl(1) ⁱⁱ	0.275 6(2)	Cd(1)-O(1)	0.234 0(4)	Cd(1)-N(1)	0.237 2(3)
N(2)-Cd(1)-N(6) ⁱ	89.62(11)	N(2)-Cd(1)-Cl(1) ⁱⁱ	88.77(10)	N(2)-Cd(1)-O(1)	92.79(12)
N(6) ⁱ -Cd(1)-Cl(1) ⁱⁱ	88.68(9)	N(6) ⁱ -Cd(1)-O(1)	89.32(12)	O(1)-Cd(1)-Cl(1) ⁱⁱ	177.45(8)
N(2)-Cd(1)-N(1)	71.58(11)	N(1)-Cd(1)-Cl(1) ⁱⁱ	92.07(9)	N(6) ⁱ -Cd(1)-N(1)	161.16(11)
Cl(1)-Cd(1)-Cl(1) ⁱⁱ	86.41(5)	O(1)-Cd(1)-N(1)	90.33(12)	O(1)-Cd(1)-Cl(1)	92.42(9)
N(2)-Cd(1)-Cl(1)	168.28(8)	N(1)-Cd(1)-Cl(1)	97.90(9)	N(6) ⁱ -Cd(1)-Cl(1)	100.94(9)

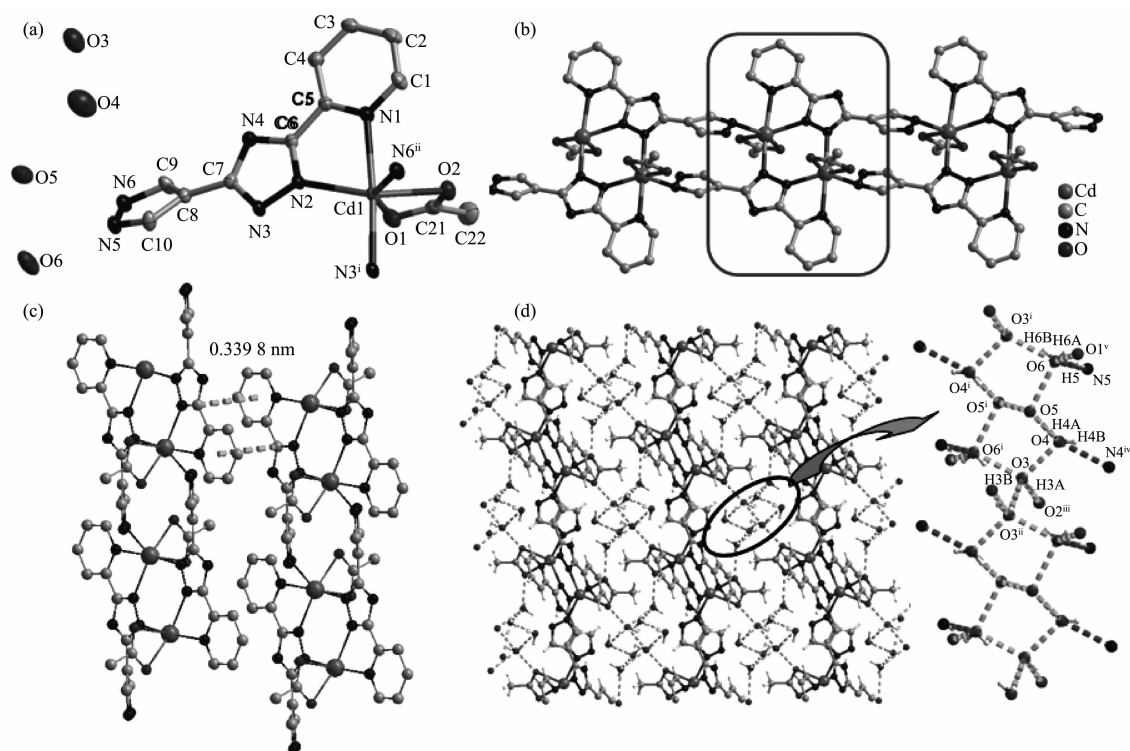
Symmetry transformations used to generate equivalent atoms: ⁱ $x, -y, 1/2+z$; ⁱⁱ $1/2-x, 1/2-y, -z$

2 Results and discussion

2.1 Crystal structures of complexes 1~2

The X-ray diffraction analysis reveals that complex **1** crystallizes in the triclinic system, space group $P\bar{1}$. There are one Cd(II) ion, one Hptp⁻ ligand, one coordinated acetate anion and three and a half free water molecules in the asymmetric unit of **1**. As shown in Fig.1a, the Cd center is six-coordinated by two O atoms (O1 and O2) from one acetate anion and four N atoms (N1, N2, N3ⁱ and N6ⁱⁱ) from three Hptp⁻ ligands

to form a distorted octahedral geometry. The apical positions are occupied by two nitrogen atom (N1, N3A) from two Hptp⁻ ligands with the N1-Cd1-N3ⁱ angle of 175.6(5) $^{\circ}$. The ligand is partial deprotonation and coordinates to three Cd(II) ions by one chelating fashion through N1 and N2 atoms and two monodentate linkages via N3, N6 atoms. As shown in Fig.1b, two asymmetric units give rise to a dinuclear secondary building unit which connected with each other to form a 1D ladder chain. Aromatic $\pi \cdots \pi$ stacking interaction between adjacent benzene rings connected the



Symmetry codes: ⁱ $-x, 2-y, 1-z$; ⁱⁱ $x, 1+y, z$ in (a); ⁱ $1-x, 1-y, -z$; ⁱⁱ $2-x, 1-y, -z$; ⁱⁱⁱ $-1+x, 2-y, 1-z$; ^{iv} $1-x, 1-y, 1-z$; ^v $-x, 1-y, 1-z$ in (d)

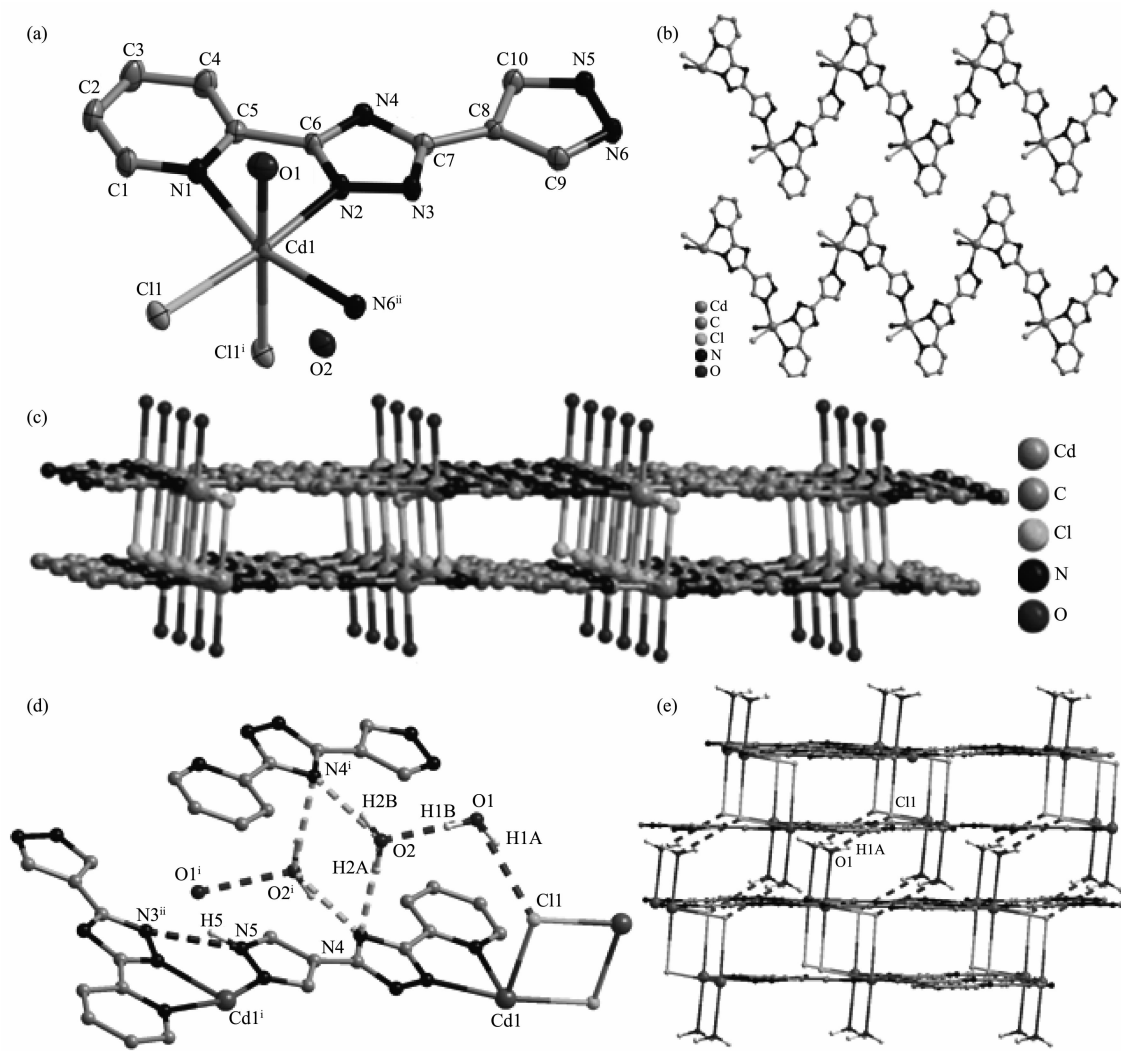
Fig.1 (a) ORTEP drawing of **1** with 30% thermal ellipsoids; (b) $[\text{Cd}_2(\text{Hptp})_2(\text{OAc})_2]$ dinuclear unit and the 1D ladder chain of **1**; (c) $\pi \cdots \pi$ stacking interactions in **1**; (d) 3D supramolecular architecture and the one dimensional water chains in **1**

chains to form a 2D supramolecular layer along the *b* axis ($\text{Cg1} \cdots \text{Cg2}$ 0.339 8 nm) (Fig.1c).

As we all know, hydrogen bonding interactions are usually important in the construction of supramolecular architectures. Exactly, double pentanuclear water cluster was formed by intermolecular $\text{O}-\text{H} \cdots \text{O}$ hydrogen bonding between the lattice water molecules located into the cavity of two adjacent layers in complex **1**. The adjacent water clusters are further expended to a water chain by hydrogen bonds of $\text{O3}-\text{H3B} \cdots \text{O3}^{\text{ii}}$ (Fig.1d). Moreover, the water chain is fixed to the structure of **1** by the strong hydrogen bonds of $\text{O4}-\text{H4B} \cdots \text{N4}^{\text{iv}}$, $\text{N5}-\text{H5} \cdots \text{O6}$ and $\text{O3}-\text{H3B} \cdots \text{O2}^{\text{iii}}$ (Fig.1d). These hydrogen bonding interactions not only

make the skeleton of the structure more stable, but also link the 2D network to form a 3D supramolecular architecture (Fig.1d).

Structural analysis show that **2** crystallizes in the monoclinic system, space group $C2/c$. As shown in Fig.2a, the asymmetric unit of **2** contains one Cd(II) ion, one chloride anion, one Htp^- , one coordinated water molecule as well as one free water molecule. Each Cd(II) ion is in a distorted octahedral environment with three nitrogen atoms from two Htp^- ligands, one oxygen atom from a coordinated water molecule, and two bridging chlorine anions. The apical positions are occupied by O1 and Cl1 ($\text{Cd1}-\text{O1}$ 0.233 2(3), $\text{Cd1}-\text{Cl1}$ 0.275 6(2) nm). The equatorial plane is completed by



Symmetry codes: ⁱ $x, -y, 1/2+z$, ⁱⁱ $1/2-x, 1/2-y, -z$ in (a); ⁱ $1/2-x, 1/2-y, -z$; ⁱⁱ $x, -y, -1/2+z$ in (d)

Fig.2 (a) ORTEP drawing of **2** with 30% thermal ellipsoids; (b) Zigzag chains in **2**; (c) 2D double layer in **2**; (d) Hydrogen bonds in **2**; (e) 3D supramolecular architecture connected by hydrogen bonds in **2**

Table 4 Hydrogen bond parameters in **1** and **2**

D-H...A	<i>d</i> (D-H) / nm	<i>d</i> (H-A) / nm	<i>d</i> (D...A) / nm	∠DHA / (°)
Complex 1				
N5-H5...O6	0.086	0.194	0.278 5(5)	169.6
O6-H6B...O3 ⁱ	0.085	0.204	0.279 9(5)	148.0
O6-H6A...O1 ⁱⁱ	0.085	0.202	0.275 5(5)	143.9
O4-H4B...N4 ⁱⁱⁱ	0.085	0.221	0.294 4(5)	145.3
O4-H4A...O5	0.085	0.194	0.276 2(8)	162.2
O5-H5A...O6	0.085	0.193	0.275 1	160.7
O5-H5B...O5	0.085	0.222	0.281 5(6)	136.5
O3-H3B...O2 ^v	0.085	0.202	0.274 9	143.6
O3-H3A...O3 ^{iv}	0.085	0.232	0.273 7	110.2
Complex 2				
N5-H5...N3 ⁱ	0.094	0.199	0.287 3(4)	154.6
O2-H2A...N4 ⁱⁱ	0.089	0.201 8	0.305 7(4)	170.8
O2-H2B...N4 ⁱⁱⁱ	0.089	0.194	0.280(4)	164.8
O1-H1A...Cl1 ^{iv}	0.085	0.236	0.316 8(3)	158.5
O1-H1B...O2 ^v	0.085	0.186	0.269 3(4)	165.4

Symmetry transformations used to generate equivalent atoms: ⁱ $-x+1, -y+1, -z$; ⁱⁱ $-x, -y+1, -z+1$; ⁱⁱⁱ $-x+1, -y+1, -z+1$; ^{iv} $-x+2, -y+1, -z$; ^v $-x+1, -y+2, -z+1$ for **1**; ⁱ $1-x, +y, 1.5-z$; ⁱⁱ $0.5+x, 0.5-y, 0.5+z$; ⁱⁱⁱ $+x, -y, 0.5+z$; ^{iv} $-x, y, -z-1/2$; ^v $x-1, y, z-1$ for **2**

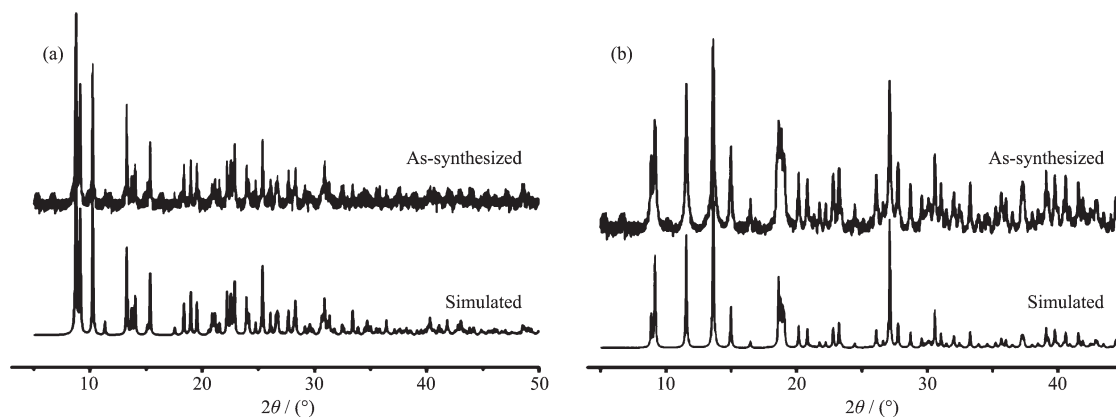
N1, N2, N6 and Cl1 with the mean deviations of 0.126 1 nm from the plane (Cd1-N1 0.237 2(3), Cd1-N2 0.226 7(3), Cd1-Cl1 0.214 8(15), Cd1-N6 0.228 5(3) nm). The Hptp⁻ ligand coordinates to two Cd(II) ions by one chelating fashion through N1 and N2 atoms and one monodentate linkage via N6 atom. As depicted in Fig.2b, the adjacent Cd(II) ions are bridged by Hptp⁻ ligands to form a 1D zigzag chain. Adjacent zigzag chains in one plane are connected by the bridging chlorine anions to form a novel 2D double layer (Fig.2c).

The hydrogen bonds also play an important role

in the construction of the supramolecular architectures of **2**. The lattice water molecules (O2) are trapped inside the gap of the 2D double layer by three kinds of powerful hydrogen bonds: O2-H2A...N4, O2-H2B...N4ⁱ and O1-H1B...O2 (Fig.2d and Table 4). The 2D layers are further expanded to a 3D network by O1-H1A...Cl1 hydrogen bonds and O1-H1B...O2 hydrogen bonds (Fig.2e).

2.2 Powder X-ray diffraction analysis

To check the phase purity of the products, powder X-ray diffraction (PXRD) experiments have been carried out for these complexes (Fig.3). The peak

Fig.3 Powder XRD pattern for **1** (a) and **2** (b)

positions of the experimental and simulated PXRD patterns are in good agreement with each other, indicating that the crystal structures are truly representative of the bulk crystal products. The differences in intensity may be owing to the preferred orientation of the crystal samples.

2.3 Thermal analysis

Thermogravimetric analysis (TGA) was carried out for complex **1** and **2** and the results are shown in Fig.4. For **1**, the weight loss of about 14.5% before 260 °C corresponds to the release of four lattice water molecules (Calcd. 15.98%). The high release temper-

ature confirms the existence of strong hydrogen-bonding interactions between water molecules and acetate anions in **1**. The TGA of **2** displays that the lattice and the coordinated water molecules are released in the same temperature range (110~205 °C) (Found 9.06%; Calcd. 9.23%), which may be attributed to the strong hydrogen bonds of O2 (O2-H2A...N4, O2-H2A...N4ⁱ and O1-H1B...O2). Then the Cl⁻ anions were loosed in the 320~440 °C range (Found 17.85%; Calcd. 18.46%) and subsequently the complex **2** decomposed.

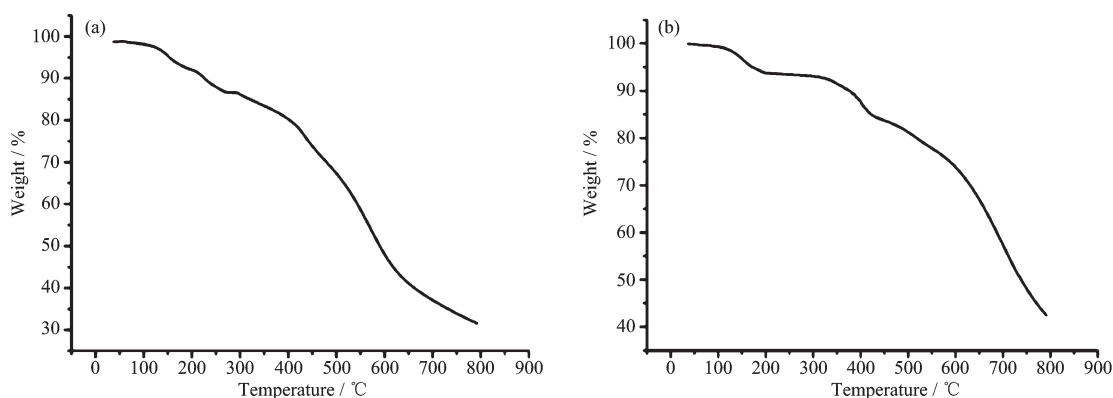


Fig.4 TGA diagram for **1** (a) and **2** (b)

2.4 Photoluminescence properties

Coordination polymers composed of d^{10} metal centres and organic ligands have been investigated to exploit their fluorescence property because of their potential applications as luminescent materials, especially those involving Cd(II) ions as coordination centres^[18-19]. Although the synthesis of the desired luminescent materials is still a challenge in this area, it is undoubted that appropriately incorporating conjugated organic ligands and anionic components into a coordination polymeric system is an efficient method to adjust luminescent properties of the materials, such as excitation/emission wavelength, intensity, lifetime, and so forth. In this study, luminescence properties of all compounds and the free ligand have been explored at room temperature in the solid state because they are virtually insoluble in most common solvents such as acetone, methanol, chloroform, benzene, water, and so forth. Upon excitation at *ca.*

386 nm, the H₂ptp ligand shows emissions at *ca.* 467 nm (Fig.5), which is assigned to $\pi \rightarrow \pi^*$ transitions. However, the strongest emissions occur at 441 nm for **1**, 426 nm for **2** upon excitation at 385 nm, respectively, showing a significant blue shift compared with the free ligand. The emissions of complexes **1**~**2** can be

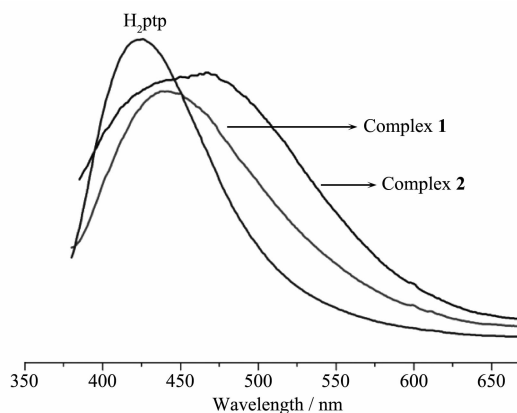


Fig.5 Solid state luminescence spectra for H₂ptp, **1** and **2** at room temperature

attributed to the ligand-to-metal charge transfer^[20-21]. The different coordination behaviors of Htp⁻ and different counter anions in the framework are probably responsible for the shift difference of the emission bands in **1**~**2**. These observations suggest that these compounds can serve as candidates for potential photoactive materials.

3 Conclusions

By assembling of Cd (II) salt and the new asymmetric rigid triazole derivatives, H₂pbt, two new Cd (II) coordination polymers has been obtained. Complex **1** shows one dimensional (1D) ladder chain, which is further extended to a two dimensional (2D) supramolecular layer via $\pi \cdots \pi$ stacking interactions. The 2D layers are further linked by hydrogen bonding to form a three dimensional (3D) supramolecular network. Complex **2** exhibits a unique 2D double layered motif which is further expanded to a 3D supramolecular structure through interlayer $\pi \cdots \pi$ stacking interactions and hydrogen bindings. In addition, the photoluminescence properties investigation suggests that these compounds can serve as candidates for potential photoactive materials.

References:

- [1] Du L T, Lu Z Y, Zheng K Y, et al. *J. Am. Chem. Soc.*, **2013**, **135**:562-565
- [2] Zhao B, Cheng P, Chen X Y, et al. *J. Am. Chem. Soc.*, **2004**, **126**:3012-3013
- [3] Liu T F, Zhang W J, Sun W H, et al. *Inorg. Chem.*, **2011**, **50**: 5242-5248
- [4] XIE Qing-Fan(解庆范), GAO Ping-Zhang(高平章), CHEN Yan-Min(陈延民). *Chinese J. Inorg. Chem.*(无机化学学报), **2014**, **30**:2382-2388
- [5] Xu Z, Meng W, Li H, et al. *Inorg. Chem.*, **2014**, **53**:3260-3262
- [6] Xiao J, Liu B Y, Wei G. *Inorg. Chem.*, **2011**, **50**:11032-11038
- [7] Nagarkar S S, Das R, Poddar P, et al. *Inorg. Chem.*, **2012**, **51**: 8317-8321
- [8] LIU Hui-Yan(刘会艳), WANG Hai-Ying(王海营), NIU De-Zhong(牛德仲), et al. *Chinese J. Inorg. Chem.*(无机化学学报), **2007**, **23**:611-614
- [9] Xu Z, Wang Q, Li H, Meng W, et al. *Chem. Commun.*, **2012**, **48**:5736-5738
- [10] Hou D C, Jiang G Y, Zhao Z. *Inorg. Chem. Commun.*, **2013**, **29**:148-151
- [11] Shi X, Wang X, Li L, et al. *Cryst. Growth Des.*, **2010**, **10**: 2490-2500
- [12] Li H X, Wu H Z, Zhang W H, et al. *Chem. Commun.*, **2007**, **47**:5052-5054
- [13] WANG Hui(王慧), GAN Guo-Qing(甘国庆), QU Yang(瞿阳), et al. *Chinese J. Inorg. Chem.*(无机化学学报), **2012**, **28**:1217-1221
- [14] Cheng J J, Chang Y T, Wu C J, et al. *CrystEngComm*, **2012**, **14**:537-543
- [15] Sheldrick G M. *SHELXS-97, Programs for X-ray Crystal Structure Solution*, University of Göttingen, Göttingen, Germany, **1997**.
- [16] Sheldrick G M. *SHELXL-97, Programs for X-ray Crystal Structure Refinement*, University of Göttingen, Göttingen, Germany, **1997**.
- [17] SADABS, Bruker AXS Inc., Madison, WI, **2004**.
- [18] Xu Z Q, Mao X J, Jia L L, et al. *J. Mol. Struct.*, **2015**, **1102**: 86-90
- [19] Li H, Cai H, Xu Z, et al. *Inorg. Chem. Commun.*, **2015**, **55**: 1-4
- [20] Li X P, Zhang J Y, Pan M, et al. *Inorg. Chem.*, **2007**, **46**: 4617-4625
- [21] Jin X H, Sun J K, Cai L X, et al. *Chem. Commun.*, **2011**, **47**: 2667-2669